Chem. Eng. Comm., 192:805–826, 2005

ISSN: 0098-6445 print/1563-5201 online
DOI: 10.1080/009864490521499

Taylor & Francis
Taylor & Francis Group

A Torus Model Containing a Sliding Well-Mixed Zone as a Way to Represent Mixing Process at Unsteady Stirring Conditions in Agitated Vessels

J.-Y. DIEULOT

Laboratoire d'Automatique et Informatique Industrielle de Lille, UMR CNRS 8021, Ecole Polytechnique Universitaire de Lille, Villeneuve d'Ascq, France

N. PETIT AND P. ROUCHON

Centre Automatique et Systèmes, École des Mines de Paris, Paris, France

G. DELAPLACE

Institut National de la Recherche Agronomique, Laboratory for Food Process Engineering and Technology, Villeneuve d'Ascq, France

This article investigates the modeling of mixing phenomena occur at unsteady stirring conditions in that agitated vessels. In particular, a new model of a torus reactor including a well-mixed zone and a transport zone is proposed. The originality of the arrangement of ideal reactors developed here is due to the time-dependent location of the boundaries between the two zones. This concept is applied to a model of the positive influence of unsteady stirring condition on a homogenization process; the model avoids mass balance discontinuity during the transitions from steady to unsteady stirring conditions.

To ascertain the reliability of the model proposed, experimental runs with highly viscous fluids have been carried out in an agitated tank. The impeller used is a nonstandard helical ribbon impeller, fitted with an anchor at the bottom. The degree of homogeneity in the tank is recorded using a conductivity method after a tracer injection.

It is shown that, for a given agitated fluid and mixing system, the parameters of the model are easy to estimate and that modeling results are in close agreement with experimental ones. Moreover, it appears that this model allows the easy derivation of the control law, which is a great advantage when optimizing the dynamics of a mixing process.

Keywords Mixing; Modeling; Nonlinear dynamics; Parameter identification; Unsteady stirring; Torus model

Introduction

High-viscosity mixing operations in batch mode are commonly encountered in chemical and food industries. The purpose of these mixing applications, which are

Address correspondence to J.-Y. Dieulot, Laboratoire d'Automatique et Informatique Industrielle de Lille, UMR CNRS 8021, I.A.A.L. Ecole Polytechnique Universitaire de Lille, 59055 Villeneuve d'Ascq, France. E-mail: dieulot@univ-lille1.fr

both time and energy consuming, is often to achieve, adequate end-product quality. However, in spite of its present wide use, the optimization of batch mixing remains an important challenge for process engineers. Depending on whether the design of the mixing system is set or not, there are different possible ways to improve mixing.

The first one is to select, for a given mixing system, the geometrical parameters that optimize the overall homogenization efficiency. Over the past few decades, this approach has been widely covered in literature. In particular, the effects of the design of the agitator and of various geometrical parameters of the mixing equipment (wall clearance, shape of the bottom, bottom clearance, number of baffles, and so on) on the efficiency of the homogenization process when stirring under steady rotational speed have been investigated. For example, one may mention studies concerning the determination of power consumption and mixing times for mixing systems equipped with close-clearance impellers such as screw or helical ribbon agitators (Tatterson, 1994; Delaplace and Leuliet, 2000; Delaplace et al., 2000a), which are known to be the best suited to achieving mixing of highly viscous media.

The second way is to consider that, for a given mixing system, the ability of a flow to homogenize viscous products can be significantly enhanced with the help of unsteady time-varying stirring methods. This approach is based on the point of view that efficient mixing in the laminar regime is related to the amount of stretching and folding generated within the tank by the agitator (Ottino, 1989; De La Villeon et al., 1998). Indeed, generally, when stirring conditions are steady, the initially designated material of fluid will follow closed streamlines in the vessel and consequently the mixing efficiency will be rather poor since such regular flows will induce a linear evolution of intermaterial area with time (Niederkorn and Ottino, 1994). However, when a suitable perturbation is superimposed on the steady velocity field, reorientation flows will appear, fluid elements will no be longer trapped by closed steady streamlines, and they will be free to move throughout chaotic flow domains. This is because the rate of stretching is higher in these flow regions, and the intermaterial area will grow faster (Niederkorn and Ottino, 1994), and higher average efficiency values will be obtained.

Although it has been shown (Ottino, 1989; Aref, 1984) over the past two decades that a time periodic velocity field applied to two-dimensional flows (pipe for example) mixes more efficiently than a steady flow, few attempts have been made to apply this approach to a batch reactor (3-D) in order to enhance the efficiency of an existing mixing device.

For example, there is a lack of systematic studies providing us with quantitative information about the conditions under which these chaotic flows are produced and their actual benefits for mixing efficiency. Consequently, the design of a sequence of flows that involves a reorientation of material elements (for instance, when periodic or co-reverse rotation of the impeller is performed) has not been clearly identified.

Another lack appears if we analyze pioneering works (Lamberto et al., 1996; Nomura et al., 1997; Yao et al., 1998) that use unsteady stirring approaches to enhance laminar mixing in batch reactors. Most of the reported examples of the improvement of three-dimensional batch mixing using unsteady rotational speed operating conditions deal with small-diameter agitators that are usually devoted to work in turbulent regimes and are not suited to batch mixing viscous fluids. In this case, the key consideration of their work was to show that periodic or co-reverse rotation of the impeller can prevent the formation of the isolated mixed regions (Metzner and Taylor, 1960) (segregated regions) occur in stirred tanks for Reynolds numbers values below 500.

From this survey, it appears clear that there is a strong need for rational studies that quantify the efficiency of a stretching process for a given mixing system. The lack of comparative knowledge of flow mixing ability does not allow the design of optimal control that would minimize the energy or time expense required to achieve a given degree of homogeneity. At the present state of the art, it is completety hopeless to try to achieve such a flow classification since it requires the entire velocity field in a stirred tank to be known and to be explicitly integrated in order to obtain the stretching required. To sum up, experimental and numerical studies of the hydrodynamics in an agitated vessel have so far failed to provide any solutions. It is, therefore, essential to design a proper flow model for such mixing processes that incorporates significant features of partially chaotic phenomena and can be used to assess the combined effects of unsteady and steady stirring approaches on mixing efficiency.

This article is a contribution to this purpose. In this work, a model is proposed to describe batch mixing of highly viscous fluids within a vessel equipped with a helical ribbon impeller at unsteady stirring conditions. The flow model is original since it is based on a torus volume composed of a plug flow and a well-mixed region with time-varying boundaries. Experimental mixing runs (for steady and unsteady stirring approaches) are used to ascertain validity and to compare the performance of this model with that of models found in literature. Note that the ultimate framework of this scientific program is to determine an optimal controller, i.e., the rotational speed profile that minimizes the mixing energy for a given mixing time. It has been chosen to discard models based on paritial differential equations for which control design might be very difficult to carry out.

Previous Literature on Flow Modeling in Batch Reactor

Many types of models can be used to characterize real flow within a batch reactor. For steady stirring approaches, Khang and Levenspiel (1976) have first shown that an agitated vessel can be modeled by a network of ideal reactors. Khang and Levenspiel's network consists of a plug flow reactor in series with a single continuous stirred tank reactor (CSTR1) with total recycling, in which the fluid flows with a constant flow rate $\dot{Q}$ (Figure 1). Assuming that both the volumes of these two ideal reactors (V_p for the plug flow reactor and V_d for the well-mixed zone) are constant and that the flow rate $\dot{Q}$ that appears in the model is proportional to the rotational speed of the impeller N, it was possible by one experimental run (one tracer injection)

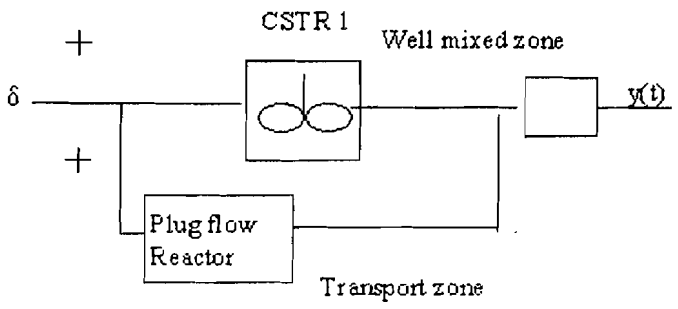

Figure 1. Recycle models proposed by Khang and Levenspiel (1976) for batch mixing.

to determine the space/time parameters of each ideal mixer (time delay θ for a plug flow reactor $\theta = V_p/\dot{Q}$ and mean residence time $T = V_d/\dot{Q}$ for a CSTR).

For unsteady stirring conditions, little information was available about the arrangement of ideal mixers that would be selected when building a model for the homogenization process. Observing experimentally that a positive variation of the impeller rotational speed enhances the mixing efficiency, Dieulot et al. (2002) have in a previous article proposed a black box model that represents the benefit (due to additional stretching) of mixing at an unsteady rotational speed by an additional CSTR (CSTR2) in the recycle loop. The final arrangement of ideal mixers chosen to describe the response curve after a tracer injection, whatever the stirring approach adopted, is shown in Figure 2. For the model proposed by Dieulot et al. (2002), the estimation of the space-time parameters of the CSTR1 and plug flow reactors was carried out using the same assumption as in the Khang and Levenspiel (1976) studies. However, space-time mathematical expressions were a little more complex since stirring conditions were non-steady and time-dependent. In particular, the additional ideal mixer (CTRS2) was chosen to relate the mean residence time to the positive variations of the rotational impeller speed. Note that with such an approach when working at steady rotational speed, the mean residence time of CSTR2 was equal to zero, which means that CSTR2 does not exist and the network of ideal mixers is reduced to the model with a recycling flow, as proposed by Khang and Levenspiel (1976) for batch mixing at steady stirring (Figure 1). As previously discussed (Dieulot et al., 2002), this model provides several advantages:

- First, it allows us to use the same network of ideal mixers to simulate the mixing performance of the agitated vessel for both the steady and unsteady approaches.
- Second, the model chosen is not too complex, since it involves only three geometrical parameters, which can be easily determined from only two experimental runs (one at constant impeller speed and the two others using unsteady rotational speed experiments).

Unfortunately this model has also its drawbacks. The worst is that is not conservative. Indeed, when the rotational impeller speed is no longer constant, an additional ideal reactor (volume due to CSTR2) appears and the mass balance in the solution is not maintained. The model cannot therefore be considered as a reliable expression of the real flow. This will give rise to the model presented in the next section. In order to respect the mass balance, it was decided not to add a further ideal reactor (such as

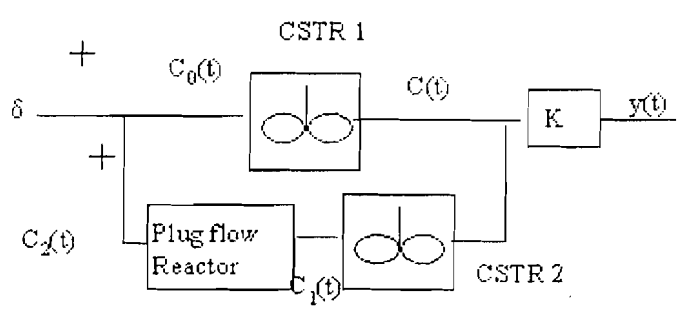

Figure 2. Recycle models proposed by Dieulot et al. (2002) to simulate the mixing process of studied mixing equipment, whatever the stirring approaches adopted (steady or non-steady).

the CSTR2 in the previous study) to account for changes in mixing conditions on transition from steady to unsteady stirring approaches. On the contrary, an attempt was carried out to model the increase in mixing efficiency due to unsteady stirring conditions both by varying the relative position of ideal zones that composed the final model and by not modifying the time parameter of each volume of the ideal zones. This was achieved by using the juxtaposition of a plug flow zone and a well-mixed zone within a torus volume with time-varying boundaries. In the following section, we will give more details the basis of the model and mathematical expressions of the space-time parameters for the ideal reactors contained in the torus volume.

Principle of the Torus Reactor Model

Consider a torus of fixed volume V divided into two ideal reactors (a stirred tank reactor of volume V_d and a plug flow zone of volume $V_p = V - V_d$) in which flows a Newtonian fluid with a uniform time-varying flow rate $\dot{Q}$ in a clockwise direction (Figure 3). In the figure $y(t)$ refers to the fluid concentration (Kg/m^3) in component y (tracer), which varies with time and space. It is assumed that the total material quantity of component y in the reactor remains constant.

The originally of the torus reactor arises from the time-dependent position of the boundaries (S_1 and S_2) that separate the two ideal flow zones. Indeed, it is assumed that when flow rate is non-steady, the relative position of the two ideal reactors is time varying. S_1 and S_2 move simultaneously with the same linear velocity and direction. Consequently, the relative volume of the two ideal reactors (V_d and V_p)

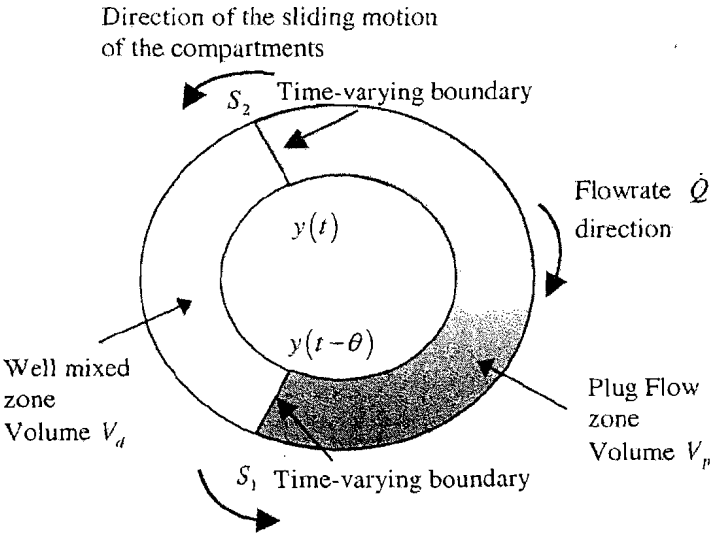

Figure 3. Sketch of torus model proposed in this study. The intensity of gray represents the concentration in then torus. S_1, S_2: time-dependent boundaries of the two compartments moving in counterclockwise direction; $\dot{Q}$: fluid flow rate in the tank, moving in clockwise direction; V_d: constant volume of the well-mixed zone for the torus volume; V_p: constant volume of the plug-flow zone for the torus volume; $y(t)$: tracer concentration in the well-mixed zone; θ: time-varying delay due to plug-flow transport.

is fixed and independent of time. In particular, it is assumed that the motion of S_1 and S_2 is controlled by the variation of flow rate that occurs in the torus volume. S_1 and S_2 move in a counterclockwise direction for positive variations of flow rate and in the opposite direction for negative fluctuations.

Note that by assuming that at every time t the flow rate $\dot{Q}(t)$ is proportional to the impeller rotational speed $N(t)$ (via α (m^3), a constant: $\dot{Q} = \alpha \cdot N(t)$), the torus model proposed is likely to describe the response curve after a tracer injection, whatever the stirring approach adopted. Indeed, for steady approaches the network of ideal mixers used to simulate the mixing process become similar to those used by Khang and Levenspiel (1976), the reliability of which has already been shown. Moreover, in the case of unsteady stirring, the model is also supposed to account for the experimental observation that an improvement in mixing occurs when a positive variation in the rotational speed is enforced. For example, in the case of a positive variation of impeller rotational speed, a fraction of liquid located in the plug flow reactor is suddenly moved into the well-mixed region. At the same time, an identical volume fraction of well-mixed liquid is released into the plug flow reactor. Overall, the mass transfer achieved using unsteady stirring is positive. Indeed, an additional nonhomogenized volume is suddenly captured by the well-mixed zone and an enhancement of mixing is expected. In fact, what happens is that the motion of the two ideal zones simulates a gain in mass transfer due to a sudden perturbation of the steady flow pattern (reorientation of fluid) induced by impeller rotational speed fluctuations.

Space-Time for the Continuous Stirred Tank Zone in the Torus Loop

The variation of volume V_d with time is zero:

$$\frac{d[V_d(t)]}{dt} = 0 \tag{1}$$

Introducing $z(t)$, the location of boundary S_1 in the torus, and S, the section of the tours, and using notations previously developed, the material balance in the well-mixed zone is:

$$\frac{d[V_d \cdot y(t)]}{dt} = \left(\dot{Q}(t) + S\frac{dz(t)}{dt}\right)y(t-\theta) - \left(\dot{Q}(t) + S\frac{dz(t)}{dt}\right)y(t) \tag{2}$$

where θ is the residence time of the particle that leaves the plug flow zone at time t.

$$V_d\frac{d[y(t)]}{dt} = \left(\dot{Q}(t) + S\frac{dz(t)}{dt}\right)(y(t-\theta) - y(t)) \tag{3}$$

Space-Time Modeling for the Plug Flow Zone in the Torus Loop

The particle that enters the plug flow zone at the instant $t = t - \theta$ and is transported with non-steady flow rate $\dot{Q}$ in a clockwise direction must go through the plug flow volume just before leaving at time t. The transport delay θ is defined by the implict Equation (4):

$$\int_{t-0}^{t} \dot{Q}(\sigma)d\sigma = V_p - \int_{t-\theta}^{t} S\frac{dz(\sigma)}{d\sigma}d\sigma \tag{4}$$

Due to the clockwise direction of flow, the plug flow volume ahead of the particle can only decrease during the route. This decrease corresponds to the second right-hand term of Equation (4).

Material Balance in the Torus Reactor

Theorem. The mass balance in the species $y(t)$ within the torus reactor defined by Equations (3)–(4) is respected.

Proof. At time t, the quantity $A(t)$ of the species y inside the reactor is the sum of that in the plug flow and the well-mixed zones,

$$A(t) = V_d\, y(t) - \int_{plug\ flow} y(t - \theta(x,t))S dz$$

where $\theta(x,t)$ is the time of residence of a particle whose abscissa in the plug flow zone is x (ranging from 0 to V_p/S). The particles at position x at time t have entered the plug flow zone at time $t - \theta(x,t)$. These particles had to travel the distance $x - \int_{t-\theta(x,t)}^{t} dz(\sigma)$, which yields the following relation that generalizes Equation(4):

$$\int_{t-\theta(x,t)}^{t} \dot{Q}(\sigma)d\sigma = Sx - \int_{t-\theta(x,t)}^{t} \frac{dz(\sigma)}{d\sigma} d\sigma$$

Now let us show that the derivative of $A(t)$ is zero.

Deriving the equation above with respect to t and z, we obtain the useful relations:

$$\dot{Q}(t) + S\frac{dz(t)}{dt} = \left(\dot{Q}(t - \theta(x,t)) + S\frac{dz(t)(t - \theta(x,t))}{dt}\right) \times \left(1 - \frac{(\partial\theta(t - \theta(x,t),x))}{\partial t}\right)$$

$$\frac{\partial\theta(x,t)}{\partial t}\left(\dot{Q}(t - \theta(x,t)) + S\frac{dz(t - \theta(x,t))}{dt}\right) = S$$

First, we calculate

$$\frac{d}{dt}\int_{plug\ flow} y(t - \theta(x,t))S dx = \int_0^{V_p/S} \dot{y}(t - \theta(x,t))\left(1 - \frac{\partial\theta(t - \theta(x,t),x)}{\partial t}\right) S dx$$

which becomes, using previous equations,

$$\frac{d}{dt}\int_{plug\ flow} y(t - \theta(x,t))S dz = \int_0^{V_p/S} \dot{y}(t - \theta(x,t)) \times \frac{\dot{Q}(t) + S\dfrac{dz(t)}{dt}}{\left(\dot{Q}(t - \theta(x,t)) + S\dfrac{dz(t - \theta(x,t))}{dt}\right)} S dx$$

$$\frac{d}{dt}\int_{plug\ flow} y(t-\theta(x,t))Sdx = \left(\dot{Q}(t) + S\frac{dz(t)}{dt}\right) \times \int_0^{V_p/S} \dot{y}(t-\theta(x,t))\frac{\partial\theta(x,t)}{\partial t}Sdx$$

and, integrating the last equation,

$$\frac{d}{dt}\int_{plug\ flow} y(t-\theta(x,t))Sdx = \left(\dot{Q}(t) + S\frac{dz(t)}{dt}\right)(y(t) - y(t-\theta(t)))$$

Replacing in the derivative of $A(t)$ yields:

$$\dot{A}(t) = \left(\dot{Q} + S\frac{dz(t)}{dt}\right)y(t-\theta) - \left(\dot{Q} + S\frac{dz}{dt}\right)y(t) + \left(\dot{Q}(t) + S\frac{dz(t)}{dt}\right)(y(t) - y(t-\theta(t))) = 0$$

which completes the proof.

Simulation Algorithm Used for the Torus Reactor

Finally, using the notations previously introduced, the whole system can be characterized by the following differential equations:

$$\begin{cases} V = V_d + V_p \\ \int_{t-\theta}^{t} \dot{Q}(\sigma)d\sigma = V - V_d - \int_{t-\theta}^{t} S\frac{dz(\sigma)}{d\sigma}d\sigma \\ V_d\frac{d[y(t)]}{dt} = \left(\dot{Q}(t) + \frac{dz(t)}{dt}\right)[y(t-\theta) - y(t)] \\ \dot{Q}(t) = \alpha \cdot N(t) \end{cases} \tag{5}$$

Assuming that the total volume of torus reactor V corresponds to the volume of the fluid agitated, the proposed system involves four unknown parameters: α, V_d, $z(t)$, and $y(t)$.

Providing two prerequisites, a simulation algorithm can be used to predict the output $y(t)$:

- The two constant parameters (α and V_d), which are not influenced by the time-dependent rotational speed, are known.
- The effects of stirring conditions $N(t)$ on boundary motions (S_1 and S_2) are established. Indeed, such knowledge will allow us to obtain $z(t)$ at each instant time. Consequently, $\theta(t)$ and then $y(t)$ can also be computers.

The assumptions used in this article concerning the evolution of $z(t)$ with stirring conditions are the following:

$$\frac{dz(t)}{dt} = k\frac{dN}{dt} \text{ with } k \text{ a positive constant} \tag{6}$$

The simulation of a system involving an input-dependent transport delay is not always trivial since the delay is defined by an implict equation. In particular, Zenger and Ylien (1994) have shown that for most flow rate fluctuations, the expression of

$\theta(t)$ cannot be obtained analytically but must be computed by numerical methods. In this work, this issue is not dealt with in detail for the sake of simplicity. More information about the computational methods used in this work can be found in the original publication (Zenger and Ylinen, 1994) or a previous one (Dieulot et al., 2002).

Finally, note that the simulation algorithm has been developed considering the toroidal model as a discrete automaton. First, the torus has been divided into a large number of cells. At every simulation step, the values of the concentration should move from one cell of the plug flow zone to the next one, using the definition of a plug flow reactor (pure transport). The concentration in the well-mixed zone can then be computed using a total mass balance and the fact that the concentrations in every cell of the zone are equal. The boundaries are then updated. The time step is variable and corresponds to the residence time in a cell, which depends on the flow rate values (rotational speed).

Material and Methods

Apparatus Used to Monitor Mixing Experiments

The mixing equipment used appears in Figure 4. During all the experiments, the level of the liquid at rest was kept constant at a 0.402 m height for a total volume of $30{\cdot}10^{-3}\,m^3$. Experiments were carried out with the helix pumping upward (counterclockwise rotation). Additional information about the flow pattern produced by the mixing system is given elsewhere (Delaplace et al., 1999, 2000a,b).

The agitated fluid is an aqueous solution of glucose with a viscosity of 1.8 Pa.s at 26°C. A controlled speed rotational viscometer (Contraves, Rheomat 30) was used to determine the Newtonian viscosity of the medium. The shear rate ranged from 01.

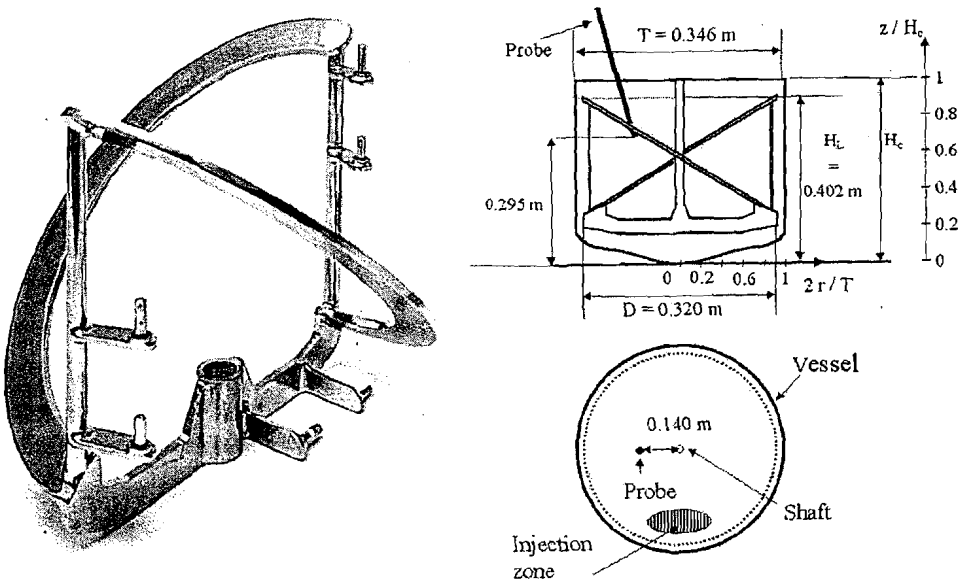

Figure 4. Photo and geometrical parameter of the mixing equipment investigated (other geometrical parameters of PARAVISC® mixing system: blade width, $w = 0.032$ m; impeller pitch, $p = 0.560$ m; impeller height; $L = 0.340$ m; tank height, $H_c = 0.443$ m).

to $500\,s^{-1}$, and the dependence of viscosity and density with temperature was taken into account.

A conductivity probe (Solea-Taccussel, type CD 78) was used to obtain the circulation curves in the vessel after a tracer injection. The signal was amplified by a converter (Type AT40, Sfere) and recorded with the help of an I/O board (PCL-812 PG, Advantech) plugged into a PC. The sampling rate was 200 Hz.

The tracer pulse injected had the same physical properties as the fluid in the tank (composition and temperature) with an additional quantity of NaCl at a concentration of 100 g/L. The incorporation was performed with the help of a pneumatic system with pistons (type DACO, PCM DOSYS) equipped with a duct (DACC 48/40, DOSYS) that held the product at the end of the pipe. This device is able to inject 72 mL (0.24% of the tank volume) of viscous tracer into the tank with an accuracy of 2%. The injection duration is a fraction of a second. This was checked by measuring a sample of the injected fluid before and after each injection, showing that the influence of the addition of salt on density and viscosity is negligible for a limited (40) number of successive trials. The volume of the tank was brought back to $30.10^{-3}\,m^3$ after each experiment. The conductivity probe and the injection locations were kept unchanged during all the experiments (Figure 4).

The I/O board allowed the operating conditions, i.e., the injection time, the departure, and the magnitude of speed variations that are enforced on the agitation system, to be controlled with precision. The rotational speed and the conductivity signal were recorded throughout the mixing process. Recording was activated three seconds before the tracer injection. Each experiment (for one set of experimental conditions) was repeated four times to ensure repeatability.

The values of the rotational speed varied from 0.16 to 1.5 rev/s. Mixing and circulation times were determined form the response signal recorded after tracer injection. The mixing time was defined as the duration needed for the signal to reach 95% of its final value (Figure 5). The circulation time was defined as the signal period

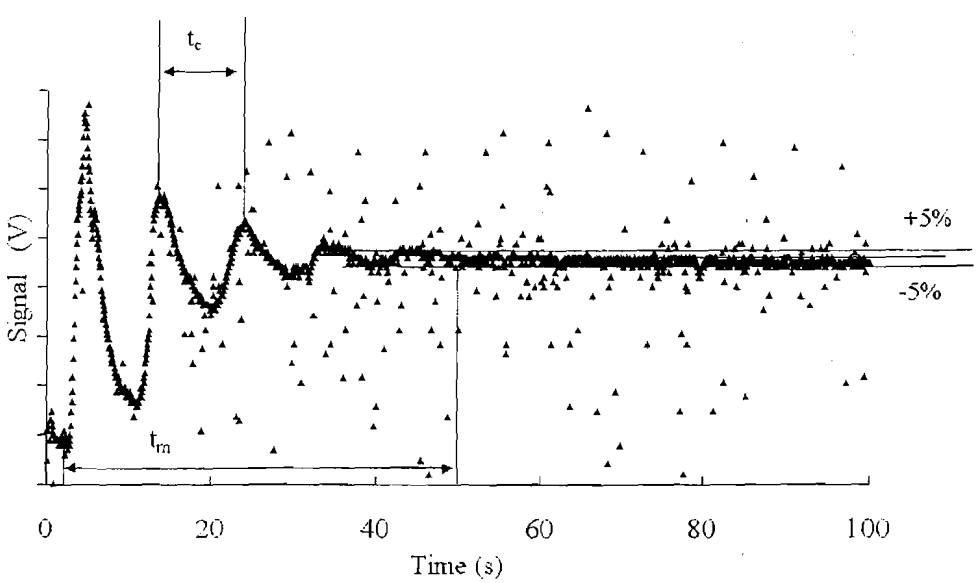

Figure 5. A typical probe response curve.

when mixing at constant impeller rotational speed (Figure 5). When the conductivity method was used, it is clear that the values of circulation and mixing times depended significantly on the location of the injection point and measurement probe. Nevertheless, for the experimental conditions tested, the local values of axial circulation times obtained are in close agreement with the global values obtained by following the movement of freely suspended particles. Moreover, global values of axial circulation times deduced from computational fluid dynamics (CFD) velocity field (Delaplace et al. 2000a, 2001) were also in close agreement with those obtained by the conductivity method.

The conductivity signals (axial circulation curves) were particularly noisy, owing to recording problems and high-frequency environmental noise (Figure 5). Filtering consisted first in the elimination of scatters. Measuring points with a derivative higher than a threshold value (empirically five times the signal derivative standard deviation) were replaced by an average value of their neighbors. The sampling period was taken to be equal to one second. This choice is important for parameter identification and has been already justified and discussed elsewhere (Delaplace et al., 1999).

Operating Stirring Conditions Tested

Table I shows the different types of operating stirring conditions tested after tracer injection. Trials 1 and 2 refer to well-known steady stirring approaches, whereas trials 3 to 8 concern unsteady stirring approaches. In the context of this article, trials 3 to 4 will be called "speed ramps," trials 5 to 7 "speed pulses," and trial 8 "speed step."

Note that, for each type of perturbation, different operating conditions were adopted (for example, various time lapses between tracer injection and the start of the impeller rotational speed fluctuations (PS)). The various operating conditions tested are also reported in Table I.

Parameter Identification: V_{d1}, α, k

The torus model proposed requires the estimation of three constant parameters, V_{d1}, α, and k (defined by Equations (5) and (6)), which depends on the characteristics of the mixing device and on the viscous media (which are constant throughout this study).

Parameters V_{d1} and α were estimated from one tracer experiment when mixing at constant impeller speed (0.667 rev/—traial number 1 in Table I).

Using the values of the parameters V_{d1} and α as previously estimated, an additional injection was performed with unsteady stirring conditions (a speed pulse, trial number 5 in Table I) in order to obtain the value of parameter k.

The set of model parameters was estimated using an optimization algorithm (Simplex method). The optimization algorithm is based on the minimization of the mean absolute error criterion defined in Equation (7).

$$\mathrm{MAE} = \frac{1}{M}\sum_{i=0}^{M-1}\left|\varepsilon(i.T_e)\right| \tag{7}$$

This criterion represent the sum of the absolute differences $\left|\varepsilon(i.T_e)\right|$ between the experimental points and the estimated points, T_e is the sampling period (one

Table I. Operating conditions (impeller rotational speed fluctuations) adopted during the mixing process after tracer injection

Trial number	Name and type of impeller rotational speed fluctuation		N_1 (rev/s)	N_2 (rev/s)	Time parameters (s)
1	Steady stirring	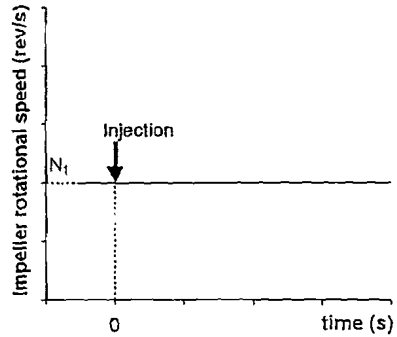	0.667	—	—
2	Steady stirring		0.833	—	—
3	Ramp speed	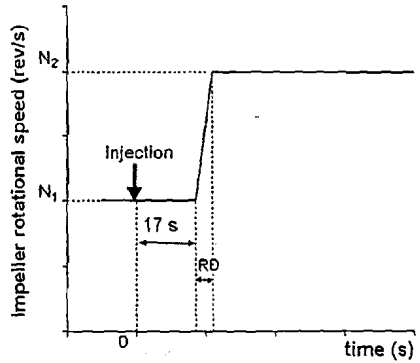	0.667	1.333	**RD** 5
4	Ramp speed		0.667	1.333	15

					PS
5	Pulse speed	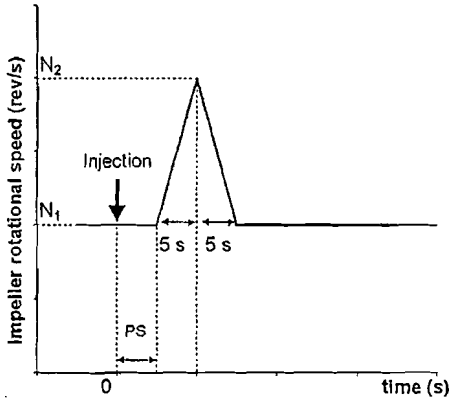	0.667	1.333	17
6	Pulse speed		0.667	1.333	10
7	Pulse speed		0.667	1.333	4
8	Step speed	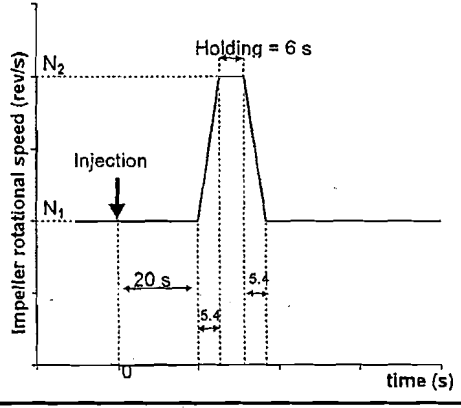	0.667	1.333	—

second), and M is the number of samples required to describe the homogenization process.

Reliability of the Model

Using different operating conditions (trials 2–4 and 6–8 in Table II) than those adopted for parameter estimation (trials 1 and 5), the validity of the model was tested. The reliability procedure consisted of comparing experimental and predicted mixing times (obtained with the help of estimated parameters). The means absolute error between experimental and model data was also computed and its value compared to those obtained for the trials used for fitting.

Results

Efficiency of Mixing Using Unsteady Stirring Conditions

The positive influence of unsteady stirring conditions on mixing efficiency is shown in Table II. It can be observed that the mixing work values required for unsteady stirring are less significant than those calculated for the mixing procedures that would give identical mixing times at constant rpm. These values of energy consumed and their determinations have already been discussed (Dieulot et al., 2002) and are not the key consideration of this work. Note simply that, as presented in previous work, depending upon the type of unsteady stirring conditions adopted, the energy savings vary form 30 to 60% and justify the introduction of time-dependent perturbations for homogenization processes.

Validity of the Model

The predictive model developed in this study was tested for our mixing equipment.

The well-mixed zone is supposed to account for the high-gradient zones, which mainly lie within the gap between the helical impeller blade and the tank wall. On the other hand, the plug flow zone refers to the axial circulation motion of the fluid within the rest of the vessel. Of course, the sum of the plug flow and the well-mixed zone volumes is equal to the total volume of the vessel.

As mentioned before, one trial at constant impeller speed (trial 1) and one run at unsteady speed (a pulse, trial 5; see Table III were necessary to determine the set of parameters of the various ideal zones. The values of the parameters estimated (supposing that the surface of a section of the torus is $10^{-1}\,m^2$) are: $V_{d1} = 6.010^{-3}\,m^3$, $\alpha = 1.6110^{-3}\,m^3$, and $k = 0.37$ m.s and were then used with other stirring conditions (see Table III) to validate the proposed model.

Examples of curve fitting obtained by this approach are given in Figures 6–11. These figures show that the estimated response curve after tracer injection is close to the experimental one despite the high noise observed for the experimental curves and the nonlinearities (such as nonperiodicity of signals, which sometimes occurs at constant impeller speeds). Moreover, in order to test the accuracy of the model, the values of measured mixing times and values calculated by the model are reported in Table III. we can note that there is close agreement between the experimental and predicted values of mixing times, whatever the stirring conditions adopted (mean error 9.2%). As previously explained, another criterion has also been computed to

Table II. Experimental mixing performance of the helical mixing system studied using various stirring conditions

	Trial 1 Steady stirring	Trial 2 Steady stirring	Trial 3 Ramp (RD = 5 s)	Trial 4 Ramp (RD = 15 s)	Trial 5 Pulse (PS = 17 s)	Trial 6 Pulse (PS = 10 s)	Trial 7 Pulse (PS = 4 s)	Trial 8 Step
Experimental mixing time (s)	80.7	72	33	38.5	60.7	58.5	65.1	53.3
Experimental mixing work (J)	627.9	937.8	793.6	763.6	510.9	525.6	385	579.7
Values of mixing work (J) for the mixing process that would give same mixing time at constant impeller rotational speed (Khang and Levenspiel (1976)	627.9	937.8	1535.5	1214.3	740.4	814.6	1035.7	980.9
Energy savings	—	—	48.3	37.1	31.0	35.5	62.8	40.9

Starting impeller rotational speed = 0.667 rev/s except trial 2.

Table III. Values of MAE and predicted values of mixing times obtained by the model for the helical mixing system studied using various stirring conditions

	Operating conditions used for parameter identification		Operating conditions used for model validation					
	Trial 1 Steady stirring N = 0.667 rev/s	Trial 5 Pulse (PS = 17 s)	Trial 2 Steady stirring N = 0.833 rev/s	Trial 3 Ramp (RD = 5 s)	Trial 4 Ramp (RD = 15 s)	Trial 6 Pulse (PS = 10 s)	Trial 7 Pulse (PS = 4 s)	Trial 8 Step
Experimental mixing time (s)	80.7	60.7	72	33	38.5	58.5	65.1	53.3
Predicted values of mixing time (s)	81.5	62.2	65.6	42.4	45.1	56.7	62.3	57.8
Values of criterion MAE (V)	0.24	0.25	0.27	0.24	0.27	0.21	0.18	0.22

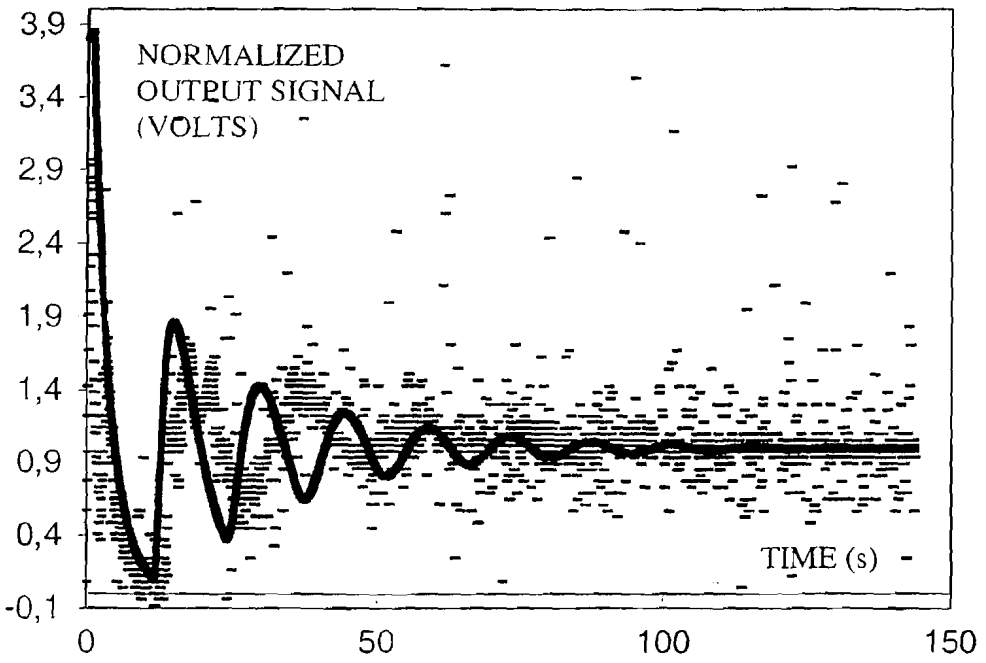

Figure 6. Predicted (solid line) and experimental (dash) circulation curve for steady speed at 40 rpm.

estimate the validity of the model: the sum of the absolute differences between the calculated and experimental outlet curves. Values of the mean absolute error (MAE) between experimental and model data are also reported in Table III.

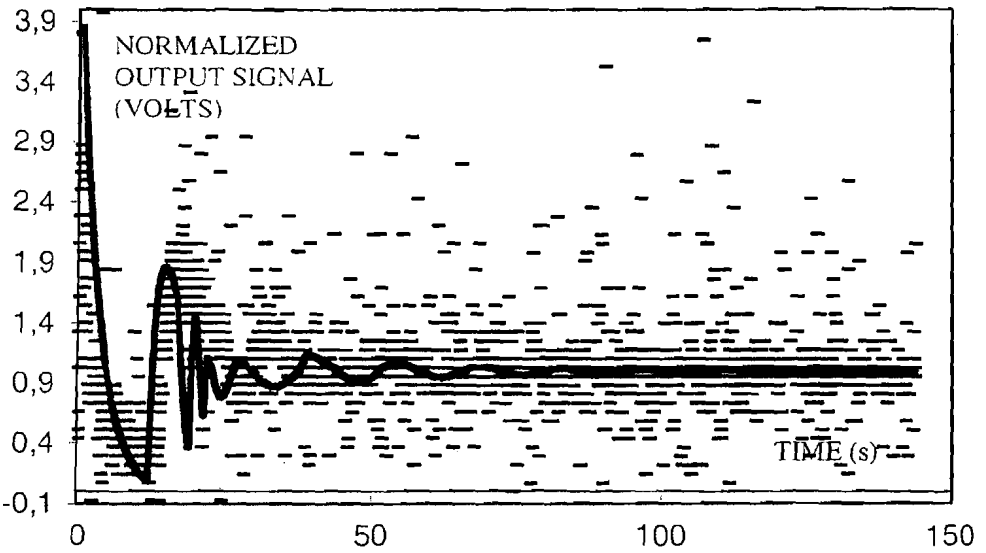

Figure 7. Predicted (solid line) and experimental (dash) circulation curve for speed pulse from 40 to 80 rpm, starting at 17 s, duration 5 s (trial 5 in Table II).

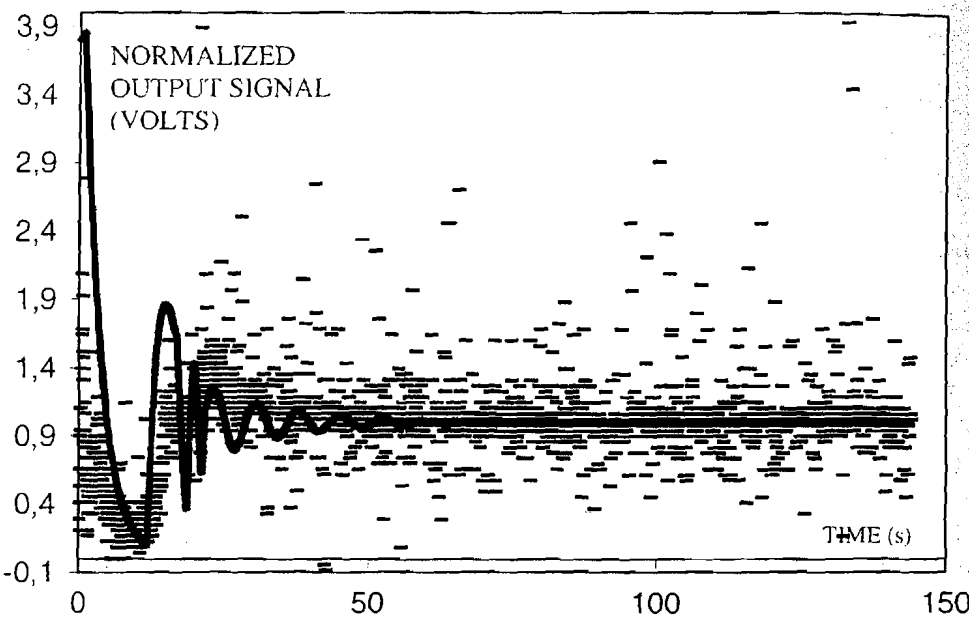

Figure 8. Predicted (solid line) and experimental (dash) circulation curve for speed ramp from 40 to 80 rmp, starting at 17 s, ramp duration RD = 5 s (trial 4 in Table II).

The values of MAE deduced from trials used for model validation (0.18–0.27) are not significantly different from those deduced from a trial used for parameter estimation (0.25).

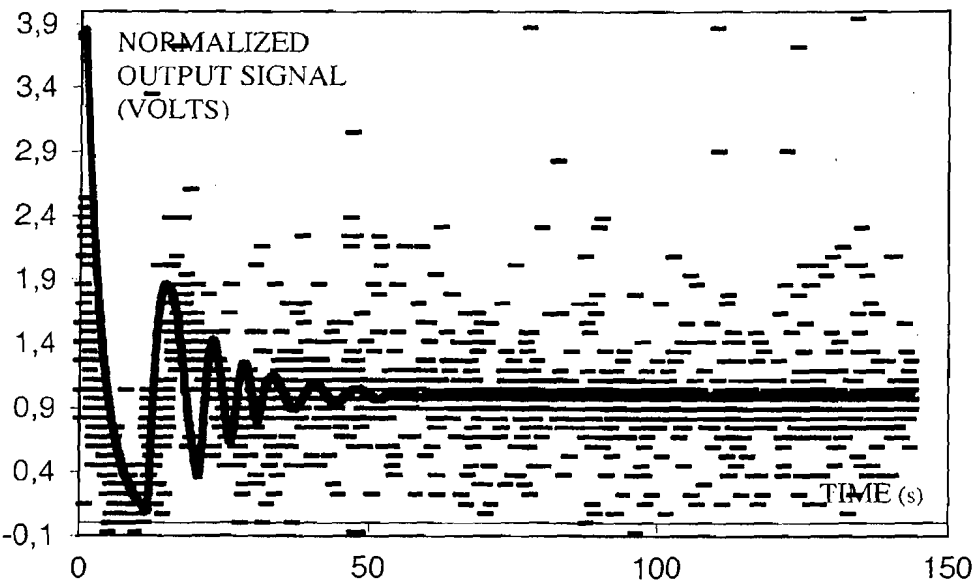

Figure 9. Predicted (solid line) and experimental (dash) circulation curve for speed ramp from 40 to 80 rmp, starting at 17 s, ramp duration RD = 15 s (trial 3 in Table II).

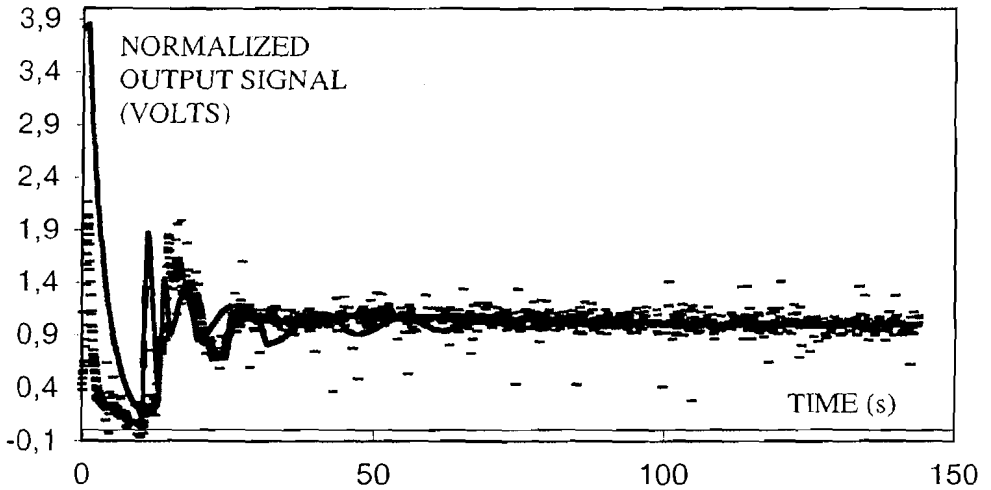

Figure 10. Predicted (solid line) and experimental (dash) circulation curve for speed pulse from 40 to 80 rmp, starting at 10 s, duration 5 s, PS = 10 s (trial 6 in Table II).

All these experimental results concerning modeling show us that it is possible to describe the mixing process that occurs under steady or unsteady stirring using the structure of the proposed model. One major advantage of the torus reactor compared to previous studies (Dieulot et al., 2002) is that the mass balance in the species within the batch reactor is respected. Note that the toroidal reactor model is not a limited concept that applies only to a specific mixing system design. On the contrary, the proposed model can be generalized to describe other mixing processes at steady or unsteady rotational speeds in stirred tanks.

In this study, our concern was only single-phase systems, and only two compartments were necessary to model the mixing phenomena (we repeat that our ultimate goal is mixing control). The use of so few compartments will indeed make it difficult

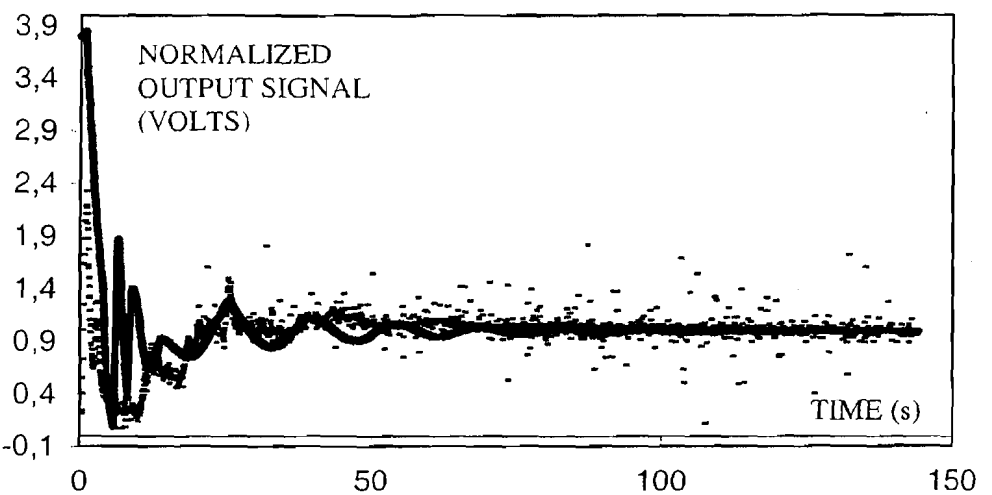

Figure 11. Predicted (solid line) and experimental (dash) circulation curve for speed pulse from 40 to 80 rmp, starting at 4 s, duration 5 s, PS = 4 s (trial 7 in Table II).

to use in multiphase mixing, such as with gas-liquid bioreactors. In this case, a model involving a network-of-zones with a large number of compartments is needed to capture the partial segregation of gas and liquid phase reagents (Rahimi and Mann, 2001; Zahradnik et al., 2001; Hristov et al., 2001) and related works.

Another motivation to use the torus reactor is to derive a control law for the rotational speed of the impeller from a mathematical equation, which optimizes the dynamics of mixing. Indeed, introducing the following change of time scale:

$$ds = \left(\dot{Q}(t) + \dot{V}_d^+\right)dt \tag{8}$$

Equations (5) and (6) become:

$$s(t) - s(t-\theta) = V_p \text{ and } V_d(U(s)) \cdot \frac{dY}{ds}(s) = Y(s-\varsigma) - Y(s) \tag{9}$$

where $\dot{Q} = U(s(t))$; $y(t) = Y(s(t))$ and ς are defined by $\varsigma = V_p(U(s-\varsigma))$.

From Equations (8) and (9), it can be seen that, if V_d is an increasing function of u, then there is a difference when $u > 0\left(\dot{V}_d^+ \neq 0\right)$ and $u < 0\left(\dot{V}_d^+ = 0\right)$, and that for $u > 0$ the new "time" $s(t)$ passes faster. Mixing is thus more efficient when the flow accelerates, which is consistent with experimental observations. This can be illustrated by considering a flow with a sawtooth profile, for which the volumes will retain their initial value after the sawtooth is completed. In a first instance, the boundary S_1 moves and V_d expands. When S_2 moves in turn and V_p expands as u decreases, the plug flow zone will move counterclockwise and will overlap an area that was previously in the well-mixed zone. The effect of $u < 0$ is thus more limited than in the case where $u > 0$.

Finally, defining ς by $W = V_d(U)$ as the control parameter and using volume balance in the torus, it can be written:

$$W \cdot \frac{dY}{ds}(s) = Y(s-\varsigma) - Y(s) \text{ and } \varsigma + V_d(U(s-\varsigma)) = V \tag{10}$$

By construction $W \in [0, V]$ and a positive solution for ς always exists when W is a continuous function of s. When the equation has several roots, ς should be chosen as the smallest. Consequently, using the torus model, an optimal solution for the control should be quite simple to obtain using algebraic methods. This will be tackled in future work.

Conclusion

A torus model has been developed to describe the mixing process at unsteady rotational speeds. The combination of ideal reactors proposed includes a well-mixed and a plug flow zone contained in a torus volume. The boundaries between the two zones vary with the flow rate (proportional to impeller rotational speed) and are supposed to represent the enhancement of mixing efficiency that is experimentally observed when using unsteady stirring conditions.

The knowledge of only three constant parameters, V_{d1}, α, and k, is required for the model proposed. Moreover, only two trials are necessary to estimate the three fixed parameters (one at constant impeller speed for V_{d1} and α, and one at unsteady rotational speed for k).

Finally, the model proposed gives close agreement between predicted and experimental circulation curves and allows us to estimate the mixing times for any kind of rotational impeller speed profile. It has been shown that the mathematical equations of the model will allow a control law for the rotational speed of the impeller to be determined.

Nomenclature

D	impeller diameter, m
H_c	tank height, m
H_L	liquid height, m
k, α	model parameters (see units in text)
L	impeller height, m
N	impeller rotational speed, rev s^{-1}
$\dot{Q}$	fluid flow rate, $m^3\ s^{-1}$
p	helical ribbon pitch, m
S_1, S_2	moving boundaries for the torus volume, m^2
t	time, s
T	tank diameter, m
T_e	sampling period used for estimation, s
t_m	mixing time, s
V	vessel or torus reactor volume, m^3
V_d	volume of the well-mixed zone for the torus volume, m^3
V_p	volume of the plug-flow zone for the torus volume, m^3
w	blade width, m
W_m	mixing work, J
$y(t)$	tracer concentration, Kg/m^3

Greek Letters

α	proportionality constant, m^3
ρ	fluid density, $kg\,m^{-3}$
θ	time-varying delay, s
μ	viscosity of Newtonian fluid, Pa s

References

Aref, H. (1984). Stirring by chaotic advection, *J. Fluid Mech.*, **143**, 1–21.

De La Villeon, J., Bertrand, F., Tanguy, P. A., Labrie, R., Bousquet, J., and Lebouvier, D. (1998). Numerical investigation of mixing efficiency of helical ribbons, *AIChE J.*, **44**(4), 972–977.

Delaplace, G. and Leuliet, J. C. (2000). Power consumption of helical ribbon impellers in highly viscous liquids—A review, *Entropie*, **227**, 10–21.

Delaplace, G., Dieulot, J.-Y., Brienne, J.-P., and Leuliet, J.-C. (1999). Détermination expérimentale et prédiction des temps de mélange pour un système d'agitation hélicoïdal, *Can. J. Chem. Eng.*, **77**, 447–457.

Delaplace, G., Leuliet, J.-C. and Relandeau, V. (2000a). Circulation and mixing times for helical ribbon impellers: Review and experiments, *Exp. Fluids*, **28**(2), 170–182.

Delaplace, G., Torrez, C., André, C., Belaubre, N., and Loisel, P. (2000b). Numerical simulation of flow of Newtonian Mixing: Proceedings, 289–296, Elsevier, Amsterdam.

Delaplace, G., Torrez, C., André, C., and Leuliet, J.-C. (2001). Tracer experiments, a way to validate computational fluid dynamic simulations in an agitated vessel, *Récents Progrés en Génie des Procédés*, **15**(79): 77–84.

Dieulot, J.-Y., Delaplace, G., Guérin, R., Brienne, J-P., and Leuliet, J. C. (2002). Laminar mixing performances of a stirred tank equipped with helical ribbon agitator subjected to steady and unsteady rotational speed, *TransIChemE*, **80**, Part A, 335–344.

Hristov, H., Mann, R., Lossev, V., Vlaev, S. D., and Seichter, P. (2001). A 3-D analysis of gas-liquid mixing, mass transfer and bioreaction in a stirred bio-reactor, *Food Bioprod. Process.*, **79**, 232–241.

Khang, S. J. and Levenspiel, O. (1976). New scale-up and design method for stirrer agitated batch mixing vessels, *Chem. Eng. Sci.*, **31**, 569–577.

Lamberto, D. J., Muzzio, F. J., Swanson, P. D., and Tonkovich, A. L. (1996). Using time-dependent RPM to enhance mixing in stirred vessels, *Chem. Eng. Sci.*, **51**(5), 733–741.

Metzner, A. B. and Taylor, J. S. (1960). Flow patterns in agitated vessels, *AIChE J.*, **6**(1), 109–114.

Niederkorn, T. C. and Ottino, J. M. (1994). Chaotic mixing of shear-thinning fluids, *AIChE J.*, **40**(11), 1782–1793.

Nomura, T., Uchida, T., and Takahashi, K. (1997). Enhancement of mixing by unsteady agitation of an impeller in an agitated vessel, *J. Chem. Eng. Jpn.*, **30**(5), 875–879.

Ottino, J. M. (1989). *The Kinematics of Mixing: Stretching, Chaos and Transport*. Cambridge University Press, Cambridge.

Rahimi, M. and Mann, R. (2001). Macro-mixing, partial segregation and 3-D selectivity yields inside a semi-batch stirred reactor, *Chem. Eng. Sci.*, **56**, 763–769.

Tatterson, G. B. (1994). *Scale Up and Design of Industrial Mixing Processes*. McGraw-Hill, New York.

Yao, W. G., Sato, H., Takahashi, K., and Koyama, K. (1998). Mixing performance experiments in impeller stirred tanks subjected to unsteady rotational speeds, *Chem. Eng. Sci.*, **53**(17), 3031–3043.

Zahradnik, J., Mann, R., Fialova, M., Vlaev, D., Vlaev, S. D., Lossev, V., and Seichter, P. (2001). A networks-of-zones analysis of mixing and mass transfer in three industrial bioreactors, *Chem. Eng. Sci.*, **56**, 485–492.

Zenger, K. and Ylinen, R. (1994). Simulation of variable delays in material transport models, *Math. Comp. Simul.*, **37**, 57–72.